Toward a theory of the general-anesthetic-induced phase transition of the cerebral cortex. I. A thermodynamics analogy

Moira L. Steyn-Ross,[1] D. A. Steyn-Ross,[1] J. W. Sleigh,[2] and Lara C. Wilcocks[1]
[1]*Department of Physics and Electronic Engineering, Private Bag 3105, University of Waikato, Hamilton, New Zealand*
[2]*Department of Anaesthetics, Waikato Hospital, Hamilton, New Zealand*
(Received 4 September 2000; revised manuscript received 10 February 2001; published 27 June 2001)

In a recent paper the authors developed a stochastic model for the response of the cerebral cortex to a general anesthetic agent. The model predicted that there would be an anesthetic-induced phase change at the point of transition into unconsciousness, manifested as a divergence in the electroencephalogram spectral power, and a change in spectral energy distribution from being relatively broadband in the conscious state to being strongly biased towards much lower frequencies in the unconscious state. Both predictions have been verified in recent clinical measurements. In the present paper we extend the model by calculating the equilibrium distribution function for the cortex, allowing us to establish a correspondence between the cortical phase transition and the more familiar thermodynamic phase transitions. This correspondence is achieved by first identifying a cortical free energy function, then by postulating that there exists an inverse relationship between an anesthetic effect and a quantity we define as cortical excitability, which plays a role analogous to temperature in thermodynamic phase transitions. We follow standard thermodynamic theory to compute a cortical entropy and a cortical ''heat capacity,'' and we investigate how these will vary with anesthetic concentration. The significant result is the prediction that the entropy will decrease discontinuously at the moment of induction into unconsciousness, concomitant with a release of ''latent heat'' which should manifest as a divergence in the analogous heat capacity. There is clear clinical evidence of heat capacity divergence in historical anesthetic-effect measurements performed in 1977 by Stullken *et al.* [Anesthesiology **46**, 28 (1977)]. The discontinuous step change in cortical entropy suggests that the cortical phase transition is analogous to a first-order thermodynamic transition in which the comatose-quiescent state is strongly ordered, while the active cortical state is relatively disordered.

DOI: 10.1103/PhysRevE.64.011917 PACS number(s): 87.19.La, 05.10.Gg, 05.70.Fh

I. INTRODUCTION

In a recent paper [1] we developed a theoretical model, based on known bulk neurophysiological processes, for the action of general anesthetics on the cerebral cortex. We assume that the cortex consists of collections of assemblies or macrocolumns. A macrocolumn is a group of $\sim 40\,000$–$100\,000$ neurons (in proportions 85% excitatory, 15% inhibitory) which act collectively within a small volume of the cortex. The effect of the general anesthetic was introduced into the model as a prolongation of the inhibitory postsynaptic potential.

We applied a stochastic formalism in which external (voltage-independent) inputs into an assembly were treated as random Gaussian fluctuations about a mean value. In the adiabatic limit in which input currents are assumed to equilibrate much faster than the average excitatory and inhibitory soma voltages h_e and h_i, we derived stochastic differential equations (Langevin equations) for h_e and h_i. By setting the time derivatives to zero, we found the stationary (or equilibrium solutions for $h_{e,i}$. When plotted as a function of the anesthetic effect λ, the graphs for the equilibrium soma voltages display the classic ''inverted-S'' phase transition form. See Fig. 1.

The graphs show that the cortex exhibits three main equilibrium regimes depending on the value of λ. For $\lambda \lesssim 0.3$, the model predicts a single stable state for the cortex which we refer to as ''seizure'' (region III), as it describes a situation of very high neuronal firing. The other extreme of a deep anesthetic effect ($\lambda \gtrsim 1.5$, the ''coma'' state) is also a stable state, but one in which neuronal firing is strongly suppressed. For intermediate values of the anesthetic effects, $0.3 \lesssim \lambda \lesssim 1.5$, the model predicts three stationary values for $h_{e,i}$. Two of these states are stable with respect to small fluctuations; we identify these stable states as ''activated'' (upper branch) and ''quiescent'' (lower branch). The activated and quiescent stable states are separated by an intermediate and unstable third state which provides a route by which the macrocolumn can make a rapid transition into the quiescent state. Transition into quiescence is increasingly probable as λ is increased beyond unity, and becomes compulsory for $\lambda \gtrsim 1.5$.

By linearizing the Langevin equations about these stationary states, we were able to employ standard stochastic methods to derive fluctuation spectra for h_e. These theoretical spectra are relevant to clinical measurements since the h_e excitatory soma voltages are believed to be the source of the scalp-detected electroencephalogram (EEG) signal. As the anesthetic effect is increased, the theoretical spectra show a reduction in median frequency coupled with a very pronounced increase in power as the upper-branch A_3 limit point of Fig. 1 is approached. This power increase is shown in Fig. 2. This increased cortical excitation at the point of induction is well known in the anesthesiology community, and is referred to as the ''biphasic'' response. The good qualitative agreement between the predicted changes in spec-

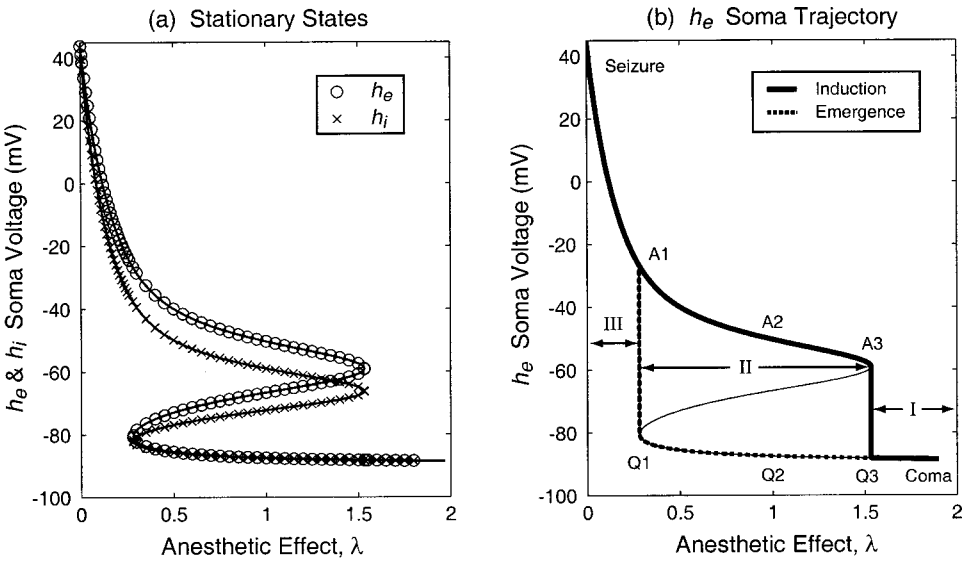

FIG. 1. (a) Model predictions for the stationary states for h_e (circles) and h_i (crosses) as a function of anesthetic effect λ. (b) In region II bounded by $A_1A_3Q_3Q_1$, for a given value of λ there are three possible values for h_e, but only two of these are stable: points lying on the upper (''active'': A_1,A_3) branch, and points on the lower (''quiescent'': Q_1Q_3) branch. For $\lambda \gtrsim 1.53$ (region I), h_e becomes single-valued and neural firing is strongly suppressed (''coma''); for $\lambda \lesssim 0.3$ (region III), h_e is again single-valued but now neural firing is maximized (''seizure''). [Based on Fig. 5 of [1], but with additional values shown locating the top-left corner seizure extremum.)

tral characteristics (frequency shift, biphasic power) and those observed in clinical measurements [2–5] provides strong supporting evidence of a physical phase transition in the cortex at the point of induction into unconsciousness.

A common characteristic of thermodynamic phase transitions is the observation of divergences in one or more parameters. The fact that EEG power appears to diverge at a critical point during induction motivates the present paper's attempt to understand the nature of this transition from a statistical mechanics perspective. Our approach will be to assert a formal correspondence between the cortical system (the macrocolumn) and a classical system, which can be described using the language and ideas of equilibrium thermodynamics.

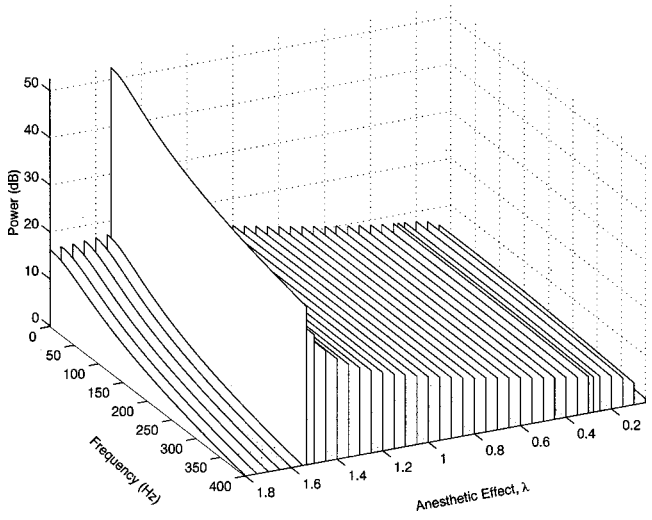

FIG. 2. Variation of spectral power for anesthesia-induction path $A_1A_3Q_3C$ of Fig. 1. Note the substantial ''slab'' of biphasic power marking the A_3 extremum immediately prior to the $A_3 \rightarrow Q_3$ jump to the lower branch. (This figure corrects a frequency-scale error on Fig. 6 of [1] which displayed a frequency unit of Hz that should have read ''kHz.'')

We need to make clear what we mean by applying the words ''thermodynamics'' and ''equilibrium'' to the phase transition of a complex biological system such as the cerebral cortex. First, we are *not* implying that the phase transition is in any way caused by changes in the thermometer-measured physical temperature of the cortex. Rather, we are asserting that the anesthetic acts in a ''temperaturelike'' manner to drive the cortex through its ''anestheto-dynamic'' phase transition into unconsciousness. In a thermodynamic transition, changes in the kinetic energy of molecules lead to altered intermolecular interactions. In the anestheto-dynamic transition, anesthetic-induced changes in neuronal synaptic responses lead to changes in the cortical information processing manifest as a loss of consciousness. The thermodynamics analogy is useful because once a suitable anesthetic-effect $\leftrightarrow$ analogous-temperature mapping has been established, we are free to use generalized thermodynamics concepts to describe the change.

Second, the equilibrium assumption is fundamental to our model: At all times the cortex never deviates far from the anesthetic-determined equilibrium points defined by the inverse-S curve of steady states shown in Fig. 1. The assumption that the cortex can be in an equilibrium state requires some justification—after all, the conventional picture of the cortex would say that it is an open, dissipative biological system which is far from equilibrium because its steady-state behavior is maintained by a continuous flux of chemical energy associated with nutrients and oxygen required for metabolic functioning. We argue that our equilibrium treatment can be justified on the basis of (1) localization and (2) scale.

(1) Local equilibrium. Glansdorff and Prigogine [6] explain how it is possible to ascribe a state of *local equilibrium* to a small mass element (in our case, the macrocolumn) which is part of a larger system (i.e., the cerebral cortex) which, as a whole, is out of equilibrium. This can be done if the local state (i.e., the soma voltage) is completely described by an equation of state which is independent of the

gradients (e.g., of chemical energy). In our case, the equation of state is represented by the Fig. 1 anesthetic-determined trajectory of soma-voltage steady states.

(2) Scale. Glansdorff and Prigogine emphasis that ''. . . the local equilibrium assumption implies that dissipative processes are sufficiently dominant to exclude large deviations from statistical equilibrium . . . . There must be sufficient dissipative 'collisions' to compensate for the effect of imposed gradients.'' For the cortex, we picture these dissipative processes as the myriad openings and closings of the millions of ion channels that service an individual neuron. These collisions occur on time scales several orders of magnitude faster than time scales of our ''mesoscale'' soma-voltage model, so the requirement for plentiful collisions is well satisfied. Further, because we are modeling at the mesoscale of the neural assembly, and not at the microscopic scale of the molecular and ionic channel processes, it is not unreasonable to replace the fine details of biological maintenance with steady-state parameters in the model (e.g., the ψ_{jk} weighting functions represent the time-averaged neurokinetics), then to treat the steady state as if it were a true equilibrium.

Given this (local) equilibrium picture, our statistical mechanics analysis of the macrocolumn proceeds as follows. We compute the Fokker-Planck equation corresponding to the Langevin equations in the adiabatic limit in which we set the time derivatives of the ''fast'' (rapidly equilibrating) variables to zero but retain their fluctuations (noise contributions) about steady state. This allows us to derive a stationary probability distribution function (PDF) $P_s(h_e,h_i,\lambda)$ for the macrocolumn. This is accomplished by decoupling the system Langevin equations (using the form of the equilibrium solutions) yielding a PDF of the form

$$P_s(h_e,h_i,\lambda)\approx P_e(h_e,\lambda)P_i(h_i,\lambda). \tag{1.1}$$

We will show that the two $P_{e,i}$ factors appearing on the right-hand side of the PDF can each be expressed as an exponential whose argument we denote by the symbol $U_{e,i}$. When plotted as a function of the anesthetic effect λ, we find that the $U_{e,i}$ map out potential hills-and-valleys curves with troughs and peaks coinciding, respectively, with the stable and unstable equilibrium points of Fig. 1. Borrowing a phenomenological technique from quantum optics [7,8], we say that the $U_{e,i}$ curves *define* potential functions which can be associated with a free energy $V_{e,i}$. The precise form of the free energy V depends on the choice of the Boltzmann function, as discussed in Sec. III B.

Continuing the thermodynamic analogy, we compute a *cortical entropy* using the Maxwell relation $S=-dV/d\Theta$, where Θ is the anesthetic-dependent analogous ''temperature,'' which we call ''excitability,'' and that we conjecture should be inversely proportional to λ. This approach is very much in the spirit of Haken's *Synergetics* work [8] in which a phenomenological free energy was inferred from a stationary Fokker-Planck equation, permitting the calculation of equivalent entropy and heat capacity in a nonequilibrium system.

In summary, this paper is concerned with establishing a thermodynamic analogy for the cortex. The cortical phase transition can then be interpreted as a particular type of phase transition, thus enhancing our predictive powers concerning anesthetic changes to brain activity, and enriching our understanding of cortical processes in general. The predictions of this paper (and that of our earlier paper [1]) rely on the applicability of the adiabatic limit. In the companion paper [9] we use numerical stochastic simulations to investigate model behaviors in this adiabatic limit, then compute another kind of macrocolumn entropy that is amenable to direct clinical measurement: spectral entropy.

Before we launch into our cortical entropy calculations, we first review the pertinent details of [1], summarizing the model that provides our defining equations of state.

II. THEORETICAL FRAMEWORK

A. Stochastic differential equations (SDEs)

Our model was described in some detail in [1]. The model is based on a set of partial differential equations (PDEs) derived by Liley *et al.* [10] which describe the time development for h_e and h_i for a neuronal aggregate. We transformed the PDEs of Liley *et al.* into stochastic differential equations (SDEs) by incorporating noise terms assumed to originate from random fluctuations in the subcortical inputs. This resulted in the following set of eight coupled SDEs:

$$\begin{bmatrix}\tau_e & 0\\ 0 & \tau_i\end{bmatrix}\frac{d}{dt}\begin{bmatrix}h_e\\ h_i\end{bmatrix}=\begin{bmatrix}h_e^{\rm rest}-h_e\\ h_i^{\rm rest}-h_i\end{bmatrix}+\begin{bmatrix}\psi_{ee}I_{ee}+\psi_{ie}I_{ie}\\ \psi_{ei}I_{ei}+\psi_{ii}I_{ii}\end{bmatrix}, \tag{2.1}$$

$$\left(\frac{d}{dt}+\gamma_e\right)^2\begin{bmatrix}I_{ee}\\ I_{ei}\end{bmatrix}=\left\{\begin{bmatrix}N_{ee}^{\beta}\\ N_{ei}^{\beta}\end{bmatrix}\mathcal{S}_e(h_e)+\begin{bmatrix}\phi_e\\ \phi_i\end{bmatrix}+\begin{bmatrix}\langle p_{ee}\rangle\\ \langle p_{ei}\rangle\end{bmatrix}\right\}G_e\gamma_e e+\begin{bmatrix}\Gamma_1(t)\\ \Gamma_2(t)\end{bmatrix}, \tag{2.2}$$

$$\left(\frac{d}{dt}+\gamma_i\right)^2\begin{bmatrix}I_{ie}\\ I_{ii}\end{bmatrix}=\left\{\begin{bmatrix}N_{ie}^{\beta}\\ N_{ii}^{\beta}\end{bmatrix}\mathcal{S}_i(h_i)+\begin{bmatrix}\langle p_{ie}\rangle\\ \langle p_{ii}\rangle\end{bmatrix}\right\}G_i\gamma_i e+\begin{bmatrix}\Gamma_3(t)\\ \Gamma_4(t)\end{bmatrix}, \tag{2.3}$$

$$\begin{bmatrix}\left(\frac{d}{dt}+\overline{v}\Lambda_{ee}\right)^2\phi_e\\ \left(\frac{d}{dt}+\overline{v}\Lambda_{ei}\right)^2\phi_i\end{bmatrix}=\overline{v}\begin{bmatrix}\left(\frac{d}{dt}+\overline{v}\Lambda_{ee}\right)\Lambda_{ee}N_{ee}^{\alpha}\\ \left(\frac{d}{dt}+\overline{v}\Lambda_{ei}\right)\Lambda_{ei}N_{ei}^{\alpha}\end{bmatrix}\mathcal{S}_e(h_e), \tag{2.4}$$

where

$$\begin{bmatrix}\Gamma_1(t)\\ \Gamma_2(t)\end{bmatrix}=\begin{bmatrix}\alpha_{ee}\sqrt{\langle p_{ee}\rangle}\xi_1(t)\\ \alpha_{ei}\sqrt{\langle p_{ei}\rangle}\xi_2(t)\end{bmatrix}G_e\gamma_e e,$$

$$\begin{bmatrix}\Gamma_3(t)\\ \Gamma_4(t)\end{bmatrix}=\begin{bmatrix}\alpha_{ie}\sqrt{\langle p_{ie}\rangle}\xi_3(t)\\ \alpha_{ii}\sqrt{\langle p_{ii}\rangle}\xi_4(t)\end{bmatrix}G_i\gamma_i e. \tag{2.5}$$

The ψ_{jk} $(j,k\in\{ei\})$ are normalized weighting functions defined by,

$$\psi_{ee}\ \frac{h_e^{\rm rev}-h_e}{|h_e^{\rm rev}-h_e^{\rm rest}|},\quad \psi_{ie}=\frac{h_i^{\rm rev}-h_e}{|h_i^{\rm rev}-h_e^{\rm rest}|},$$
$$\psi_{ei}=\frac{h_e^{\rm rev}-h_i}{|h_e^{\rm rev}-h_i^{\rm rest}|},\quad \psi_{ii}=\frac{h_i^{\rm rev}-h_i}{|h_i^{\rm rev}-h_i^{\rm rest}|}. \tag{2.6}$$

The terms $I_{ee},I_{ie},I_{ei},I_{ii}$ represent intracortical neuronal inputs averaged over the assembly. The coupling strength between cells is determined by sigmoid functions $\mathcal{S}_e(h_e)$, $\mathcal{S}_i(h_i)$,

$$\mathcal{S}_e(h_e)=\frac{\mathcal{S}_{e,\max}}{1+\exp[-g_e(h_e-\theta_e)]},$$
$$\mathcal{S}_i(h_i)=\frac{\mathcal{S}_{i,\max}}{1+\exp[-g_i(h_i-\theta_i)]}. \tag{2.7}$$

In addition to sigmoid-modulated spike input from the neural mass, there are long-range (cortico-cortical) spike input contributions (ϕ_e,ϕ_i) from distant excitatory assemblies, plus soma-voltage-independent spike inputs $(p_{ee},p_{ie},p_{ei},p_{ii})$ from exogenous or external sources labeled, for convenience, as *subcortical*, and pictured physiologically as nonspecific input from the brain stem. We assume that noise arises solely in the subcortical sources, and we ignore noise entering via the cortico-cortical connections from distant assemblies.

The four $\langle p_{jk}\rangle$ subcortical sources appearing in Eqs. (2.2) and (2.3) represent the average value of each subcortical input. The four Γ terms defined in Eq. (2.5) contain noise sources $\xi(t)$ which provide the random fluctuations in the subcortical inputs. These $\xi(t)$ are Gaussian white-noise sources that have zero mean and are δ correlated,

$$\langle\xi_\eta(t)\rangle=0,\quad \langle\xi_\eta(t)\xi_{\eta'}(t')\rangle=\delta_{\eta\eta'}\delta(t-t'). \tag{2.8}$$

Each noise source is scaled by a multiplicative factor of the form $\alpha_{jk}\sqrt{\langle p_{jk}\rangle}$. The α_{jk} are dimensionless scale factors introduced to ensure the fluctuations are always small. [This is a technical refinement to our Eqs. (2.9) of [1] which, while it does not alter our theoretical development, it does become significant when attempting to solve the equations via stochastic simulation; refer to the companion paper [9] for further details.]

We introduced the effect of general anesthetic into the model by modulating the inhibitory neurotransmitter rate constant,

$$\overline{\gamma}_i=\frac{\gamma_i}{\lambda},$$

where λ is a multiplicative scaling factor assumed to be proportional to the anesthetic concentration, so that $\lambda=1$ corresponds to no anesthetic effect, and an increase in λ corresponds to an increase in the anesthetic amount (a decrease in the γ_i rate constant).

The stochastic equations (2.1)–(2.4) define our model of the cortex. Table I lists the numerical values and definitions for the equation parameters and constants.

B. Equilibrium solutions

In [1] we derived the equilibrium solutions for the macrocolumn. We solved Eqs. (2.1)–(2.4) with $d/dt=0$ and the noise terms set to zero. In this long-time limit we found the Fig. 1 stationary curves for the variations of h_e and h_i as a function of λ. This inverted-S figure is suggestive of a classical phase transition. This interpretation was confirmed by a stability analysis which showed that the upper and lower branches are stable with respect to perturbations, whereas the middle branch is unstable. Thus, if we start the system on the (high-firing, active) upper branch, and steadily increase the anesthetic amount λ, the soma voltage will slide along the upper branch until the turning point A_3 is reached. At this point the macrocolumn is forced to make a jump transition to the (low-firing, quiescent) lower branch. Conversely, if the system is started on the lower branch, then reductions in λ cause the soma voltage to slide to the left until the turning point Q_1 is reached, whereupon an upwards transition to the high-firing branch occurs.

We have run stochastic simulations of Eqs. (2.1)–(2.4). See companion paper [9] for details. The simulations show that the presence of subcortical noise allows the macrocolumn to switch between stable states (activated $\leftrightarrow$ quiescent) at other than the transition λ values (λ_{A3} or λ_{Q1}). The likelihood of state switching diminishes as the amplitude of the noise is reduced, and increases as the A_3 and Q_1 turning points are approached.

C. Langevin equations in adiabatic limit

Inspection of the various time scales for the $h_{e,i}$ soma voltages and the four $I_{jk(\{j,k\}\in\{e,i\})}$ input currents [Eqs. (2.1)–(2.4)] showed that it was reasonable to assume that the input currents would equilibrate much faster than the soma voltages. This justified a simplification in which we adiabatically eliminated the currents (details in [1]), giving the following reduced set of stochastic differential equations for the soma voltages alone,

$$\frac{d}{dt}\begin{bmatrix}h_e\\h_i\end{bmatrix}=\begin{bmatrix}F_1(h_e,h_i)\\F_2(h_e,h_i)\end{bmatrix}+\begin{bmatrix}\Gamma_e(t)\\\Gamma_i(t)\end{bmatrix}, \tag{2.9}$$

where the drift terms are

$$F_1(h_e,h_i)=\{h_e^{\rm rest}-h_e)+\psi_{ee}[(N_{ee}^{\alpha}+N_{ee}^{\beta})\mathcal{S}_e(h_e)+\langle p_{ee}\rangle]G_e e/\gamma_e+\lambda\psi_{ie}[N_{ie}^{\beta}\mathcal{S}_i(h_i)+\langle p_{ie}\rangle]G_i e/\gamma_i\}/\tau_e, \tag{2.10a}$$

$$F_2(h_e,h_i)=\{(h_i^{\rm rest}-h_i)+\psi_{ei}[(N_{ei}^{\alpha}+N_{ei}^{\beta})\mathcal{S}_e(h_e)+\langle p_{ei}\rangle]G_e e/\gamma_e+\lambda\psi_{ii}[N_{ii}^{\beta}\mathcal{S}_i(h_i)+\langle p_{ii}\rangle]G_i e/\gamma_i\}/\tau_i, \tag{2.10b}$$

TABLE I. Symbol definitions and given values for model constants.

Symbol	Description	Value	Unit
e,i	(as subscript) excitatory, inhibitory cell populations		
$h_{e,i}$	population mean soma voltage		mV
$\tau_{e,i}$	membrane time constant	0.040, 0.040	s
$h_{e,i}^{\text{rest}}$	cell resting potential	$-70,-70$	mV
$h_{e,i}^{\text{rev}}$	cell reversal potential (Nernst potential)	$45,-90$	mV
$I_{ee,ie}$	total $e\to e, i\to e$ ''current'' input to excitatory synapses		mV
$I_{ei,ii}$	total $e\to i, i\to i$ ''current'' input to inhibitory synapses		mV
$\psi_{jk(j,k\in\{e,i\})}$	weighting factors for the I_{jk} inputs		
$p_{ee,ie}$	exogenous (subcortical) spike input to e population	1100, 1600	s^{-1}
$p_{ei,ii}$	exogenous (subcortical) spike input to i population	1600, 1100	s^{-1}
$\alpha_{jk(j,k\in\{e,i\})}$	weighting factors for fluctuations in p_{jk} spike inputs	0.1	
$\phi_{e,i}$	long-range (cortico-cortical) spike input to e,i populations		s^{-1}
$\Lambda_{ee,ei}$	characteristic cortico-cortical inverse-length scale	0.40, 0.65	$(\text{cm})^{-1}$
EPSP, IPSP	excitatory, inhibitory postsynaptic potential		mV
$\gamma_{e,i}$	neutrotransmitter rate constant for EPSP, IPSP	300, 65	s^{-1}
$G_{e,i}$	peak amplitude of EPSP, IPSP	0.18, 0.37	mV
e	[e.g., Eqs. (2.5) and (2.10)] base of natural logarithms	2.718 28 . . .	
$N_{ee,ei}^{\beta}$	total number of local $e\to e, e\to i$ synaptic connections	3034, 3034	
$N_{ie,ii}^{\beta}$	total number of local $i\to e, i\to i$ synaptic connections	536, 536	
$N_{ee,ei}^{\alpha}$	total number of synaptic connections from distant e populations	4000, 2000	
$\bar{v}$	mean axonal conduction speed	700	cm s^{-1}
$S_e(h_e)$, $S_i(h_i)$	sigmoid function mapping soma voltage to firing rate		s^{-1}
$S_{e,\max}, S_{i,\max}$	maximum value for sigmoid function	1000, 1000	s^{-1}
$\theta_{e,i}$	inflection-point voltage for sigmoid function	$-60,-60$	mV
$g_{e,i}$	sigmoid slope at inflection point	0.28, 0.14	$(\text{mV})^{-1}$

and the corresponding diffusion terms are

$$\Gamma_e(t)=\{\psi_{ee}\alpha_{ee}\sqrt{\langle p_{ee}\rangle}\xi_1(t)G_e e/\gamma_e + \lambda\psi_{ie}\alpha_{ie}\sqrt{\langle p_{ie}\rangle}\xi_3(t)G_i e/\gamma_i\}/\tau_e, \quad (2.10c)$$

$$\Gamma_i=\{\psi_{ei}\alpha_{ei}\sqrt{\langle p_{ei}\rangle}\xi_2(t)G_e e/\gamma_e + \lambda\psi_{ii}\alpha_{ii}\sqrt{\langle p_{ii}\rangle}\xi_4(t)G_i e/\gamma_i\}/\tau_i. \quad (2.10d)$$

In [1] we linearized these equations about the equilibrium state defined by the inverse-S curve (Fig. 1), then used standard stochastic methods to obtain the fluctuation spectra for h_e as a function of λ shown in Fig. 2. In [9] we compare these theoretical spectra against those obtained from numerical simulation of the adiabatically simplified equations (2.9)–(2.10).

D. Fokker-Planck equation

The results of [1], as summarized in Secs. II B–II C of the present paper, predict that the cortex will undergo a phase transition as it ''freezes'' into unconsciousness. In order to explore the underlying nature of this transition, we choose to follow a statistical mechanics path which requires us to derive probability distribution functions P_e and P_i for the excitatory and inhibitory neuron populations for the macrocolumn. We generate the $P_{e,i}$ by calculating the Fokker-Planck equation equivalent to the Langevin equations of the preceding section,

$$\frac{\partial P(h_e,h_i,t)}{\partial t} = -\frac{\partial}{\partial h_e}[F_1(h_e,h_i)P(h_e,h_i,t)] - \frac{\partial}{\partial h_i}[F_2(h_e,h_i)P(h_e,h_i,t)] + \frac{1}{2}\frac{\partial^2}{\partial h_e^2}[D_1(h_e,h_i)P(h_e,h_i,t)] + \frac{1}{2}\frac{\partial^2}{\partial h_i^2}[D_2(h_e,h_i)P(h_e,h_i,t)]. \quad (2.11)$$

The $D_{1,2}$ are the diffusion (noise) terms defined by

$$\langle\Gamma_e(t)\Gamma_e(t')\rangle = D_1\delta(t-t'), \quad (2.12a)$$

$$\langle\Gamma_i(t)\Gamma_i(t')\rangle = D_2\delta(t-t'). \quad (2.12b)$$

E. Stationary distribution functions

In order to compute equilibrium parameters (such as entropy) using a statistical mechanics framework, we require

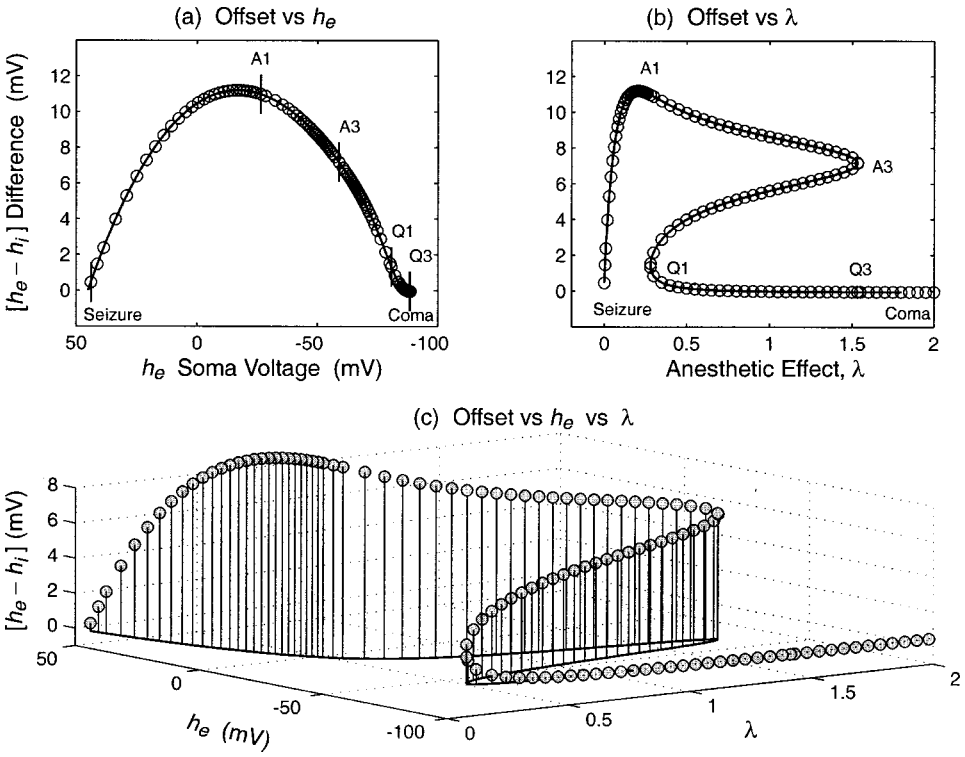

FIG. 3. Equilibrium values for h_i expressed as a λ-dependent offset from h_e: $\Delta = h_{e,0} - h_{i,0}$. The h_i values become more similar to h_e at the seizure and coma extremes. Labels correspond to those shown in Fig. 1.

the stationary distribution function $P_s(h_e, h_i)$. This is found by setting $d/dt = 0$ in Eq. (2.11). In general, for multivariate systems, an analytic expression for P_s is only obtainable when the ''potential conditions'' are satisfied (see Gardiner [11]). The (h_e, h_i) two-variable cortical system does not satisfy the potential conditions. However, an approximate solution for P_s is achievable if we use the equilibrium values of Fig. 1 to decouple Eq. (2.11) into two independent equations, one for h_e alone and a second for h_i alone. Inspection of Fig. 1 shows that, at equilibrium, the λ dependence of h_e and h_i is rather similar: the curves are almost coincident on the bottom branch, become distinct on the middle and upper branches, then converge again as they approach the top-left seizure corner. So it is reasonable to express the locus of equilibrium values of h_i as an h_e-dependent offset from the matching locus of equilibrium values of h_e,

$$h_{i,0} = h_{e,0} - \Delta(h_e), \tag{2.13}$$

where the offset term $\Delta(h_e)$ is obtained numerically from the Fig. 1 stationary curves, and is shown in Fig. 3 plotted as a function of h_e and of λ. We will assume that the $\Delta(h_e)$ offset formula, which is exact for the locus of equilibrium points, can also be applied to points nearby which are very close to equilibrium, so generalize Eq. (2.13) to read

$$h_i = h_e - \Delta(h_e). \tag{2.14}$$

This generalization is equivalent to making a Taylor expansion about equilibrium and requiring that the first-order term in the expansion, the gradient $(\partial\Delta/\partial h_e)_{(\mathrm{eq})}$, be small. Examining Fig. 3(a) we see that the absolute value of the slope is generally less than ~ 0.2, except along the unstable branch A_3Q_1 and in the vicinity of the jump points A_3 and Q_1; and also approaching seizure point S where the slope has magnitude ~ 0.35. For these regions, Eq. (2.14) will not be very accurate, but this is of little consequence for the stationary distribution function curves, since it is the locations of the distribution maxima and minima that are of prime interest, and for these points the equation is exact. (The inaccuracies in the distribution curves will manifest as shape errors *between* turning points, and might compromise calculations for first-passage times, but this is not the focus of our present work.)

Applying the offset relationships decouples the original Langevin equations (2.10a) into two independent, stochastic equations of motion, one for h_e and one for h_i, leading to two independent Fokker-Planck equations which are expected to be valid for points close to equilibrium,

$$\frac{\partial \tilde{P}_e(h_e,\lambda,t)}{\partial t} = -\frac{\partial}{\partial h_e}[\tilde{F}_1(h_e,\lambda)\tilde{P}_e(h_e,\lambda,t)] + \frac{1}{2}\frac{\partial^2}{\partial h_e^2}[D_1(h_e,\lambda)\tilde{P}_e(h_e,\lambda,t)], \tag{2.15a}$$

$$\frac{\partial \tilde{P}_i(h_i,\lambda,t)}{\partial t} = -\frac{\partial}{\partial h_i}[\tilde{F}_2(h_i,\lambda)\tilde{P}_i(h_i,\lambda,t)] + \frac{1}{2}\frac{\partial^2}{\partial h_i^2}[D_2(h_i,\lambda)\tilde{P}_i(h_i,\lambda,t)], \tag{2.15b}$$

where the overtilde variables are defined

$$\tilde{P}_e(h_e,\lambda,t)\equiv P_e(h_e,h_e-\Delta,\lambda,t),$$

$$\tilde{P}_i(h_e,\lambda,t)\equiv P_i(h_i+\Delta,h_i,\lambda,t),$$

$$\tilde{F}_1(h_e,\lambda)\equiv F_1(h_e,h_e-\Delta,\lambda),$$

$$\tilde{F}_2(h_i,\lambda)\equiv F_2(h_i+\Delta,h_i,\lambda).$$

Equations (2.15) represent an uncoupled pair of single-variable systems, so it is now possible to solve for the steady-state (long-time limit) $\overline{P_e},\overline{P_i}$ probability distributions. Following the procedures outlined in Chap. 5 of Gardiner [11], we attend to the boundary conditions by setting the ''probability currents'' equal to zero at $h_{e,i}=h_i^{\rm rev}=-90$ mV (lower bound for soma voltage), and at $h_{e,i}=+45$ mV (upper bound) and arrive at the following stationary solutions:

$$\overline{P}_e(h_e,\lambda)=\frac{\mathcal{N}_1}{D_1(h_e,\lambda)}\exp\left[2\int_{-90}^{h_e}\frac{\tilde{F}_1(h_e',\lambda)}{D_1(h_e',\lambda)}dh_e'\right] \tag{2.16a}$$

$$=\frac{\mathcal{N}_1}{D_1(h_e,\lambda)}\exp[-U_1(h_e,\lambda)] \tag{2.16b}$$

$$=\mathcal{N}_1\exp[-U_e(h_e,\lambda)] \tag{2.16c}$$

and

$$\overline{P}_i(h_i,\lambda)=\frac{\mathcal{N}_2}{D_2(h_i,\lambda)}\exp\left[2\int_{-90}^{h_i}\frac{\tilde{F}_2(h_i',\lambda)}{D_2(h_i',\lambda)}dh_i'\right] \tag{2.17a}$$

$$=\frac{\mathcal{N}_2}{D_2(h_i,\lambda)}\exp[-U_2(h_i,\lambda)] \tag{2.17b}$$

$$=\mathcal{N}_2\exp[-U_i(h_i,\lambda)], \tag{2.17c}$$

where we have moved the $D_{1,2}$ diffusion term from the outside denominator of Eqs. (2.16b) and (2.17b) into the exponential of Eqs. (2.16c) and (2.17c), so that

$$U_e=U_1+\log_e(D_1),\quad U_i=U_2+\log_e(D_2), \tag{2.18}$$

and where the normalization constants are defined by

$$\mathcal{N}_1^{-1}=\int_{-90}^{+45}\exp[-U_e(h_e,\lambda)]dh_e, \tag{2.19a}$$

$$\mathcal{N}_2^{-1}=\int_{-90}^{+45}\exp[-U_i(h_i,\lambda)]dh_i. \tag{2.19b}$$

The definite integrals in Eqs. (2.16)–(2.19) are evaluated numerically. The stationary probability distribution function for the total system of excitatory and inhibitory neurons in the macrocolumn is given by the product

$$P_s(h_e,h_i,\lambda)=\overline{P}_e\overline{P}_i, \tag{2.20}$$

which follows because the excitatory and inhibitory distributions have been decoupled and therefore made independent.

We refer to the U_e defined in Eq. (2.18) as the excitatory *potential function*, since its negative gradient $-\partial U_e/\partial h_e$ is interpretable as a force that drives the excitatory neuron voltage (a parallel comment applies to U_i). This idea becomes clearer after inspecting Fig. 4 which shows how the $U_{e,i}$ potential functions vary with soma voltage $h_{e,i}$. The points on these curves at which the gradient is zero are the ''zero-force'' or equilibrium coordinates. The stability or otherwise of a given equilibrium point is determined by the sign of the curvature in the region immediately bracketing the point. Thus if the equilibrium point lies at the bottom of a potential valley (positive curvature), any small deviations away from the local minimum will be opposed by a force acting to restore the equilibrium, making it stable. The converse is true for the equilibrium point at the top of a potential hill (region of negative curvature): a small perturbation away from the peak will produce a force tending to enhance the perturbation, so the equilibrium there will be unstable.

Figures 4(a)–4(g) show graphs of $U_{e,i}$ as a function of $h_{e,i}$ for the seven representative values of λ shown in 4(h), the last panel of the figure. These seven slices provide a coarse sweep through regions III (seizure), region II (upper branch), and into region I (coma) of Fig. 1.

We observe that the extrema of the $U_{e,i}$ potential functions coincide with the equilibrium soma voltages highlighted by the vertical lines marked on Fig. 4(h). For example, in Fig. 4(a), U_e exhibits a single valley minimum whose (λ,h_e) coordinate belongs to the upper-left ''seizure'' corner of the equilibrium soma trajectory in Fig. 4(h). This is consistent with the vertical slice through this coordinate [labeled ''*a*'' in Fig. 4(h)] cutting the h_e trajectory once only, implying that for $\lambda=0.25$ only a single equilibrium state is possible. The potential function is a minimum here, so this state is stable.

In Fig. 4(b) for $\lambda=0.50$, three well-defined extrema have developed (two unequal valleys separated by small hill), corresponding to three distinct steady-state solutions and therefore three intersections on the *b* slice of Fig. 4(h). Only the two valley-point equilibria (upper branch at $h_e=-40$ mV and lower branch at $h_e=-85$ mV) are stable, while the mid-branch equilibrium point, defined by the potential-function peak (at $h_e=-73$ mV) that separates the two valleys, is unstable. In principle, the macrocolumn could sit delicately balanced at the top of this hill, but given the slightest nudge would ''slide'' off the hill to nestle into one of the adjacent valleys.

The relative depth of the two valleys changes as λ varies, indicating that the probability of occupation also changes with λ. For $\lambda<1$, the upper (high-firing) branch is more likely; while for $\lambda>1$ the lower (low-firing) branch is favored. For $\lambda\approx1$, both stable-branch values for h_e are equally likely; and if there are perturbations of sufficient magnitude to overcome the potential hill, then there is the possibility that the macrocolumn could repeatedly switch between the upper- and lower-branch stable states.

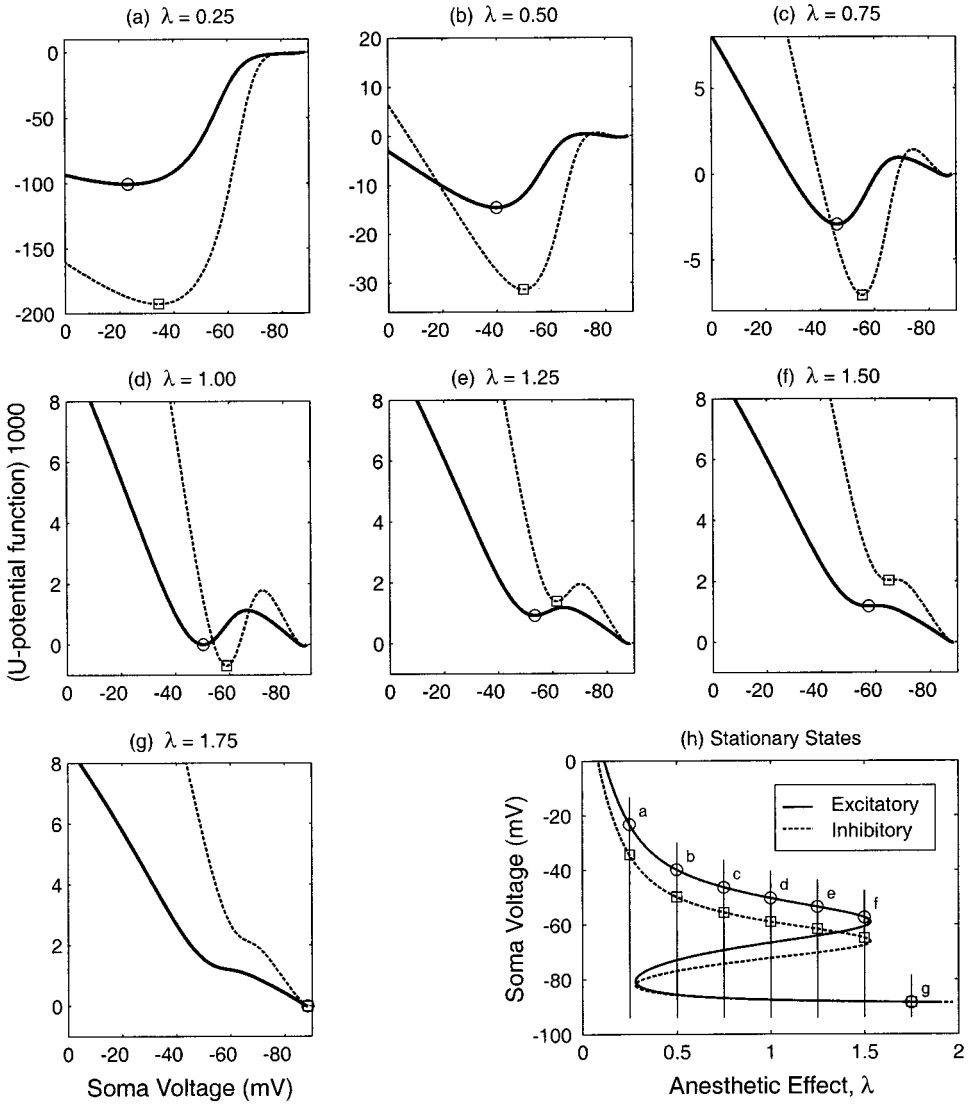

FIG. 4. (a)–(g) $U_{e,i}$-potential functions for seven representative values of λ. Solid curve: U_e; dashed curve: U_i. (h) Copy of Fig. 1 showing the seven vertical slices through the stationary-state trajectory which were used to evaluate the displayed U-functions. Circles: h_e; squares: h_i. (b)–(f) show two valleys separated by a hill; the valleys belong to the stable upper (high-firing) and lower (low-firing) branches of the trajectory curve, while the hill belongs to the unstable midbranch. Each of the labeled points in (h) maps to a valley point (local minimum) in the correspondingly labeled figure. Note that for $\lambda=1$, the two valleys are approximately symmetric. The cortical state ''rides'' the upper-branch valley as the U-curve is distorted by the anesthetic, until the cortical state is ''tipped out'' into unconsciousness in (g).

We note that these $U_{e,i}$ curves are indistinguishable from those for $U_{1,2}$ (not shown here), i.e., the locations of the valleys and hills are practically unchanged by the folding of the $D_{1,2}$ diffusion divisors into the exponentials of Eqs. (2.16b) and (2.17b).

In statistical thermodynamics, it is the Helmholtz free energy that is minimized when the system is in equilibrium. The fact that our $U_{e,i}$ potential functions have minima which correctly locate the stable equilibria leads us to suggest that these potential functions behave like Helmholtz free energy functions for the macrocolumn. We expand on this idea in the following section.

III. A STATISTICAL MECHANICS TREATMENT OF THE CORTEX

A. Philosophy

In a series of papers (see [12,13] and references therein) Ingber develops a statistical mechanics formalism of neocortical interactions. He adopts a ''bottom-up'' approach which starts at the microscopic level of synaptic interaction. His theoretical distribution function for the cortex is the conditional probability that a mesocolumn (essentially equivalent to our macrocolumn) will fire, given its interaction with other mesocolumns and its previous history of firings. Ingber's model successfully describes the formation of short-term memory, and is consistent with EEG data generated during selective attention tasks.

Our model has a more ''top-down''philosophy in that the mean-field equations and associated stationary probability distribution $P_s(h_e,h_i,\lambda)$ are a *macro*state description of the cortex. By this we mean that the computed $h_{e,i}$ values are to be regarded as representing soma-voltage averages over the $\sim$85 000 excitatory and $\sim$15 000 inhibitory neurons comprising the macrocolumn. Thus it is not possible for a mean-field model to identify the detailed microscopic states or *micro*states of the macrocolumn. (By ''microstate'' we mean the particular electrostatic configuration of soma voltages which, when summed, give the whole-macrocolumn voltage $h_{e,i}$.) However, if the underlying microstate description of the cortex were known, then the macrostate picture could be derived from it, in the same way that the $PV=nRT$ macrodescription of an ideal gas is derivable from the Boltzmann distribution of its microstates.

TABLE II. Proposed mapping between thermodynamics theory and the macrocolumn model of the cortex.

Thermodynamic space	Cortical space
Temperature, T	Excitability, Θ
Internal energy, E	Internal energy of macrocolumn, $E_{e,i}$
Helmholtz free energy, $V=E-TS$	Cortical free energy, $V_{e,i}=E_{e,i}-\Theta S_{e,i}$
Entropy, $S=-(\partial V/\partial T)$	Cortical entropy, $S_{e,i}=-(\partial V_{e,i}/\partial\Theta)$
Heat capacity, $C=T(\partial S/\partial T)$	Cortical ''heat'' capacity, $C_{e,i}=\Theta(\partial S_{e,i}/\partial\Theta)$
Latent heat, $T\Delta S$	Cortical latent ''heat,'' $\Theta\Delta S_{e,i}$

We will use this macroscopic picture to construct a statistical mechanics description of the anesthetic-induced cortical phase transition. We proceed by deriving a (phenomenological) free energy function V. The ''free energy'' concept is very useful in statistical mechanics as its negative rate change with temperature gives entropy: $S=-\partial V/\partial T$. But this step will require us to identify carefully exactly what is meant by the ''temperature'' of the cortex; by cortical ''temperature'' we do *not* mean the physical temperature measured with a thermometer. In the next section we present a line of argument, based on the idea of a canonical ensemble, to enable identification of a plausible cortical temperature analog.

B. Identifying a free energy function for the cortex

The construction of our statistical mechanics theory is motivated by the obvious similarities between the form of the $U_{e,i}$ potential functions of Fig. 4 and the potential-well description of phase transitions common in quantum optics [14]. For a quantum optics system described in terms of a parameter x, Lugiato and Bonifacio [7] write the stationary probability distribution $P_s(x)$ (usually the solution of a Fokker-Planck or Master equation) in the form

$$P_s(x)=\mathcal{N}\exp[-V(x)/k_0] \quad \text{(Lugiato and Bonifacio)}, \tag{3.1}$$

where $\mathcal{N}$ is a normalization constant, and k_0 is a constant introduced to ensure dimensional consistency. The quantity $V(x)$ plays the role of a ''generalized free energy'' [7,15]. Haken [8] follows a similar approach in his Fokker-Planck treatment of an analogous phase transition, but in his exponential term the denominator is the product of Boltzmann's constant k_B and a parameter he identifies as an equivalent temperature T,

$$P_s(x)=\mathcal{N}\exp[-V(x)/k_BT] \quad \text{(Haken)}, \tag{3.2}$$

which is very suggestive of the Boltzmann distribution. The assertion in Eqs. (3.1) and (3.2) that $V(x)$ is a free energy is justified phenomenologically on the grounds that the extrema of V locate the equilibrium states.

In both of these quantum-optics models, the diffusion-noise term is constant. In our cortical model, the diffusion has a weak $h_{e,i}$ dependence, but this dependence seems not to challenge our posited $U_{e,i}\leftrightarrow$ free energy analogy, since the extrema of $U_{e,i}$ coincide with the stationary values of $h_{e,i}$ for a given λ. Therefore we postulate that there exists a formal equivalence between the probability density functions (PDFs) of Eqs. (3.1) and (3.2) and the cortical PDF of Eqs. (2.16c) and (2.17c), and we assume that the cortical phase transition can be described in a space which is dual to that of statistical thermodynamics. The proposed dual-space mapping is set out in Table II; the various elements of this table will be discussed as the paper proceeds.

Equating the cortical potential function U from Eqs. (2.16c) or (2.17c) first with exponential argument of Eq. (3.2) (Haken form), then with the exponential argument of Eq. (3.1) [Lugiato and Bonifacio (LB) form], we obtain two alternative thermodynamic $\leftrightarrow$ cortical mappings for the free energy of the cortex,

$$U(x)\equiv V(x)/k_BT$$
$$\Rightarrow V_{\mathrm{H}}(h_{e,i})=k_B\Theta U(h_{e,i}) \quad \text{(Haken)}, \tag{3.3a}$$

$$U(x)\equiv V(x)/k_0$$
$$\Rightarrow V_{\mathrm{LB}}(h_{e,i})=k_0U(h_{e,i}) \quad \text{(Lugiato and Bonifacio)}. \tag{3.3b}$$

From Table II and Eqs. (3.3a) and (3.3b), it will be apparent that for the cortical system we have introduced the symbol Θ, which we define to be *cortical excitability*, and which, as we show using plausibility arguments developed later in the paper, plays a role in the cortex analogous to that of temperature T in thermodynamic systems. We will show that excitability Θ is inversely related to anesthetic effect λ. This (λ,Θ) mapping provides the crucial link between the cortical general-anesthetic phase transition and the world of thermodynamic phase transitions, and allows us to apply the concepts and tools of thermodynamic critical phenomena (e.g., entropy, heat capacity, and, in principle, critical exponents, universality) to the cortical transition.

C. Neurological canonical ensemble

In the absence of stimulus, a neuron will relax to its *resting potential*. In our model, this voltage is set to -70 mV (i.e., the interior of the neuron is 70 mV more negative than the outside medium). A neuron is said to be *hyperpolarized* if its soma voltage is below (more negative than) the resting potential, and *depolarized* if the voltage is above this value. The neuron cannot fire until its soma potential is raised to a threshold value which in our model is set at -60 mV. A voltage impulse arriving at the neuron is classified as *inhibitory* if it tends to make the soma voltage more negative and therefore less likely to reach threshold, and *excitatory* if it raises the soma voltage towards (or above) threshold. These

inhibitory and excitatory events occur at the synapse, effected via the release of neurotransmitters which selectively open channels to allow the passage of certain ions.

Most commonly used general anesthetic agents act by enhancing the effect of the GABA (γ-aminobutyric acid, the predominant inhibitory neurotransmitter in the cerebral cortex) neurotransmitter. This chemical increases the chloride ion currents at the postsynaptic GABAa receptor complex by allowing the Cl^- channels to remain open for longer, causing the neuron to become hyperpolarized and therefore inhibited [16,17]. At the level of individual postsynaptic GABAa/Cl^- channels, the increase in the GABA-stimulated Cl^- current is proportional to the fractional increase in the time that the channel is in the open state. We model this enhancement of channel conductance as a prolongation of the inhibitory postsynaptic potential (IPSP) (or more precisely, as a reduction in the IPSP rate constant γ_i) assumed proportional to anesthetic concentration.

Ingber [12] describes neuronal interactions in terms of a given neuron receiving quanta of chemical postsynaptic stimulation from other neurons. Each quantum consists of thousands of molecules of neurotransmitter which drive the chemically gated postsynaptic potential. Ingber goes on to suggest that one may define a cortical PDF (probability distribution function) which will '' . . . describe the distribution of electrical polarization caused by chemical quanta impinging on the postsynaptic membrane.''

This distribution of electrical polarizations determines the internal energy E of the macrocolumn system. Since the effect of anesthetic is to alter the gate opening times, thereby changing the net polarization of the macrocolumn, it is clear that the anesthetic sets the macrocolumn internal energy. Thus we paraphrase Ingber's statement to read as follows: ''For a given prolongation of the inhibitory post-synaptic potential, there exists a cortical PDF defining the microscopic distribution of soma voltages corresponding to a fixed value of internal energy.''

Such a picture has strong parallels with classical statistical mechanics distribution function derived from the *canonical ensemble*. A canonical ensemble describes a system s_0 of N particles in contact with an infinitely large heat reservoir R maintained at constant temperature T. The internal energy E of the system s_0 depends on the distribution of particles over their allowed energy states E_j. The most likely distribution is found by maximizing the PDF subject to the two constraints: N is fixed; E is fixed. The second constraint is historically associated with the undetermined Lagrange multiplier β, and for thermodynamic systems is found to be precisely related to temperature: $\beta = 1/k_B T$.

For the anesthetic-dampled cortex, the infinite reservoir is the milieu of general anesthetic in the blood stream which sustains the neurons of the macrocolumn. The concentration of the anesthetic can be taken as an externally set constant, since the time scale on which it varies ($\gtrsim$ tens of milliseconds) is very much longer than the relaxation time scales of the macrocolumn ($\sim$ tens of milliseconds). The anesthetic concentration, via the IPSP prolongation factor λ, sets the polarization state [equilibrium soma voltage (h_e^0, h_i^0) on the reverse-S of Fig. 1] and therefore the internal energy. As in the classical canonical picture, there are two constraints: N, the number of neurons in the macrocolumn is fixed (this assumption is implicit in the model: refer to the four N^β constants in Table I); and the internal energy E is fixed by the anesthetic concentration. If the cortical PDF were known, then, in principle, the most likely distribution of polarization microstates could be found by minimizing the PDF with respect to these two constraints.

Thus the heat reservoir, which sets the temperature T of the classical thermodynamic system, has been replaced in the biological system by a blood-circulation reservoir of fixed anesthetic concentration which perfuses the cortex, setting its IPSP prolongation factor λ. However, it is obvious that T and λ are *not* analogs: an increase in λ (via an increase in anesthetic concentration) causes the macrocolumn to become more hyperpolarized and therefore more ordered, whereas increasing the temperature of a thermodynamic system has a randomizing, disordering effect. This is made clearer by considering a true thermodynamic system which has persuasive similarities to the cortical phase transition: the ferroelectric phase transition.

D. Ferroelectric analogy

Consider the temperature-driven first-order phase change which occurs in ferroelectric materials such as barium titanate ($BaTiO_3$) and Rochelle salt ($KNaC_4H_4O_6 \cdot 6H_2O$) [18–20]. At temperatures below transition temperature $T_0 = 112\,^\circ C$, the $BaTiO_3$ crystal exhibits a net spontaneous electric polarization. This dipole moment exists independently of any external electric field. When the crystal is heated to a second transition temperature $T_1 = 122\,^\circ C$, its structure suddenly changes from tetragonal to cubic and the spontaneous dipole moment disappears, the crystal remaining nonpolar at all higher temperatures. At intermediate temperatures $T_0 < T < T_1$, the crystal exhibits *thermal hysteresis*, i.e., the crystal can exist in either polar or nonpolar form, depending on its thermal history. If the crystal was heated from below T_0, it will retain its polar state until temperature T_1 is reached, whereupon the polarization will suddenly and discontinuously collapse to zero. If the crystal was cooled from above T_1, it will remain unpolarized until the lower transition temperature T_0 is reached, at which point its lattice structure will spontaneously change and a dipole moment will suddenly appear.

The precise definition of the Curie point T_c ($= 120\,^\circ C$ for $BaTiO_3$) for a ferroelectric is that temperature at which the free energy wells for the polar and nonpolar states have equal depth, indicating that at that temperature both the polar and nonpolar states are equally likely [21]. The Curie point is analogous to the $\lambda = 1$ point on the cortical free energy diagrams of Fig. 4(d). In common usage, the Curie point is taken to mean the polarized $\rightarrow$ unpolarized transition temperature (i.e., $T_c \equiv T_1$ for the $BaTiO_3$ ferroelectric). In Table III we list some parallels between the ferroelectric and macrocolumn systems.

In the ferroelectric, temperature is a measure of the thermal motion which tends to destroy the polarization order. For the cortex, we define *excitability*, Θ, as the analog of

TABLE III. Parallels between ferroelectric and cortical macrocolumn systems.

Ferroelectric crystal	Cortical macrocolumn
Polar (ferroelectric) state	Hyperpolarized (quiescent) state
Nonpolar state	Depolarized (active) state
Increased temperature → loss of polarization order	Increased excitability → loss of hyperpolarization order

thermodynamic temperature which provides the randomizing disturbance tending to destroy the hyperpolarization order of the quiescent macrocolumn. For our model, excitability is, in some sense, oppositely proportional to cortical inhibition as quantified by the IPSP prolongation factor λ. We investigate several plausible (Θ,λ) mappings in the next section.

E. Relating anesthetic effect to cortical excitability

In our model, for $\lambda \gtrsim 1.53$, the macrocolumn must reside on the low-firing quiescent branch. As the anesthetic concentration is increased, the duration of the inhibitory postsynaptic potential (IPSP) is prolonged, producing greater inhibition and reduced neuronal firing. Increased anesthetic depth λ corresponds to reduced cortical excitability Θ, so λ and Θ are inversely related. In the $\lambda \to \infty$ limiting case of extreme anesthesia, there can be no activity in the presence of an infinitely prolonged IPSP, so $\Theta = 0$ in this extreme frozen limit. This point is our absolute-zero ''temperature'' at which all neurons are fully hyperpolarized.

For the emergence trajectory, Θ will increase as the hyperpolarization ordering diminishes with reductions in λ, and more neurons become depolarized (able to fire). With sufficient reduction in λ, the macrocolumn will eventually reach the seizure extremum (top-left corner of Fig. 1) at which point all neurons are fully depolarized and firing maximally, since $\lambda = 0$ means that the IPSP has zero duration so there is no inhibitory restraint on the macrocolumn firing activity. At this seizure extremum, cortical excitability will have its maximum value $\Theta_{\max}$. From a biological energy resources perspective, it is reasonable to argue that $\Theta_{\max}$ will have a large but finite value, while from a mathematical modeling perspective one might argue that $\Theta_{\max} \to \infty$ as $\lambda \to 0$ and then avoid the finite resources problem by asserting that $\lambda = 0$ is a model abstraction which will never occur in practice. In either case, we seek a mapping whose model predictions for entropy change are not unduly sensitive to the finiteness or otherwise of $\Theta_{\max}$.

The mathematical equation relating Θ to λ is unknown, but based on the foregoing discussion a plausible mapping would have the following properties:

(i) $\Theta \to 0$ as $\lambda \to \infty$ (deep coma).

(ii) Θ is a monotonic decreasing function of λ.

(iii) $\Theta \to \Theta_{\max}$ as $\lambda \to 0$ (extreme seizure), where $\Theta_{\max}$ may be finite or infinite.

Two of the simplest inverse relationships that satisfy these criteria are

$$\Theta_{\mathrm{I}} = c_0 / \lambda^{c_1} \tag{3.4a}$$

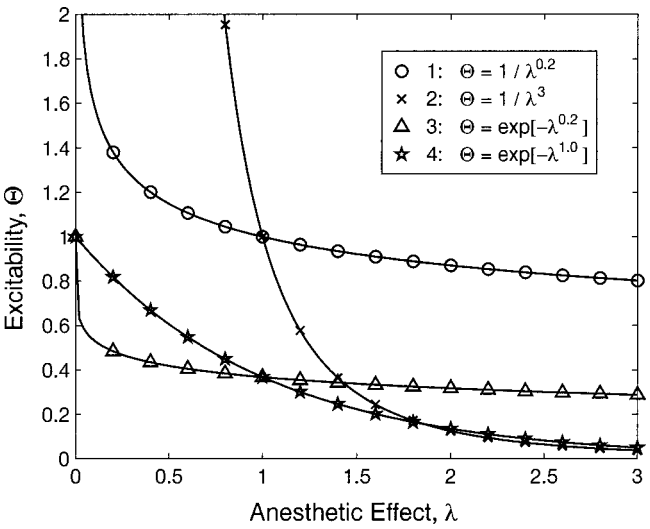

FIG. 5. Plausible excitability Θ versus anesthetic effect λ mappings. Curves 1 and 2 have unbounded excitability (''temperature'') as $\lambda \to 0$; curves 3 and 4 have finite excitability at $\lambda = 0$.

and

$$\Theta_{\mathrm{II}} = \Theta_{\max} \exp(-c_0 \lambda^{c_1}), \tag{3.4b}$$

where c_0 and c_1 are positive constants. Both functions decay smoothly to zero as $\lambda \to \infty$; for the $\lambda \to 0$ seizure extreme, $\Theta_{\mathrm{I}} \to \infty$ while $\Theta_{\mathrm{II}} \to \Theta_{\max}$, a finite maximum value. For definiteness and simplicity, we will set $c_0 = 1$, $\Theta_{\max} = 1$, and only the c_1 exponent will be altered. Figure 5 shows sample Θ-vs-λ mappings for $c_1 = 0.2$ (curves 1 and 3), $c_1 = 3$ (curve 2), and $c_1 = 1.0$ (curve 4). Curves 1 and 2 correspond to infinite activity at $\lambda = 0$ (i.e., Θ_{I} mapping), while curves 3 and 4 have finite activity $\Theta = \Theta_{\max}$ at $\lambda = 0$ (i.e., Θ_{II} mapping).

F. Cortical entropy

Applying the Eq. (3.4) ''temperature'' mappings first to the Haken potential form, Eq. (3.3a), then to the Lugiato and Bonifacio form, Eq. (3.3b), we obtain four candidate expressions for cortical entropy,

$$S_{\mathrm{I,\,Haken}} = k_B \left(\frac{\lambda}{c_1} \frac{\partial U}{\partial \lambda} - U \right), \tag{3.5a}$$

$$S_{\mathrm{II,\,Haken}} = k_B \left(\frac{\lambda^{1-c_1}}{c_0 c_1} \frac{\partial U}{\partial \lambda_U} \right), \tag{3.5b}$$

$$S_{\mathrm{I,\,LB}} = k_0 \frac{\lambda^{1+c_1}}{c_0 c_1} \frac{\partial U}{\partial \lambda}, \tag{3.5c}$$

$$S_{\mathrm{II,\,LB}} = k_0 \frac{\lambda^{1-c_1}}{c_0 c_1 \Theta_{\max}} \exp(c_0 \lambda^{c_1}) \frac{\partial U}{\partial \lambda}, \tag{3.5d}$$

where, for example, Eq. (3.5c) was derived by applying the Maxwell relation $S = -\partial V / \partial \Theta$ to the Lugiato and Bonifacio potential form $V = k_0 U$ and using the chain rule

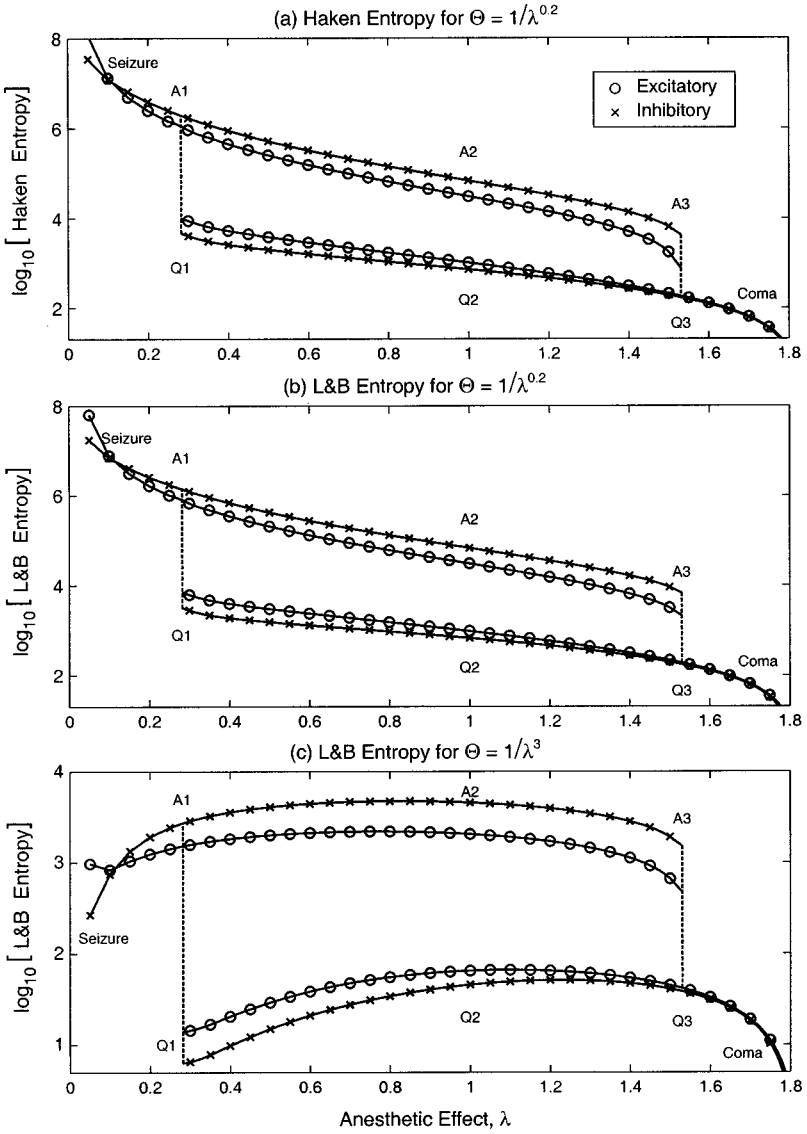

FIG. 6. Theoretical cortical entropy curves for the excitatory and inhibitory neural populations of the macrocolumn as a function of anesthetic effect. Assumed excitability (''temperature'') mapping is $\Theta = 1/\lambda^{c_1}$. (a) Haken form, $c_1 = 0.2$. (b) Lugiato and Bonifacio form, $c_1 = 0.2$. (c) Lugiato and Bonifacio form, $c_1 = 3$.

$$S_{\mathrm{I,\,LB}} = -\frac{\partial V}{\partial \Theta_{\mathrm{I}}} = -k\frac{\partial U}{\partial \Theta_{\mathrm{I}}} = -k\frac{\partial U}{\partial \lambda}\frac{\partial \lambda}{\partial \Theta_{\mathrm{I}}} = -k\frac{\partial U}{\partial \lambda}\Big/\frac{\partial \Theta_{\mathrm{I}}}{\partial \lambda} \tag{3.6}$$

with the Θ_{I} mapping giving the partial-derivative result

$$\frac{\partial \Theta_{\mathrm{I}}}{\partial \lambda} = -c_0 c_1/\lambda^{1+c_1}.$$

Graphs showing the λ dependence of the Haken and LB entropies appear in Fig. 6. All three graphs assume the type-I temperature mapping $\Theta = 1/\lambda^{c_1}$ (the type-II mappings give qualitatively similar results, so they are not shown here), with $c_1 = 0.2$ for graphs (a) and (b), and $c_1 = 3$ for graph (c). Note that for the smaller value of c_1, the Haken and LB entropy graphs are very similar, showing a maximum entropy in the top-left corner (seizure), and minimum entropy in the bottom-right corner (coma). The upper (active) and lower (quiescent) branches are separated by step discontinuities at A_3 (induction point), and at Q_1 (emergence point).

Inspection of Eqs. (3.5a)–(3.5c) shows that the Haken and LB forms will give entropy curves which become more alike for small c_1. This is because the potential gradient $\partial U/\partial\lambda$, which is scaled by $1/c_1$, will tend to dominate the U-potential term. For large c_1, the entropy curves become dissimilar. However, the presence of the subtractive U term in the Haken form places an upper bound on the maximum permissible value for c_1: we found that for $c_1 \gtrsim 0.4$ the Haken entropy becomes negative on the upper branch when $\lambda \gtrsim 1.4$. Since we require entropy to be always positive (reaching zero only in the limit of perfect order), then the range of permissible power-law exponents for the Θ-vs-λ mapping is limited to $0 < c_1 \lesssim 0.4$ for Haken entropy.

The absence of the U subtraction in the LB form means that in principle there is no upper bound for the c_1 exponent in the LB entropy expression. We have selected $c_1 = 3$ as a representative ''large'' exponent value since this produces a LB entropy curve [Fig. 6(c)] which has strong qualitative similarity to the theoretical spectral entropy curves presented in our companion paper [9]. Compared with the small-c_1 entropy graphs of Figs. 6(a) and 6(b), the large-c_1 graph 6(c)

shows a significantly different profile: the position of maximum entropy has shifted from the top-left seizure corner to a position on the upper branch in the vicinity of $\lambda = 1$. This feature suggests that the normal conscious state is associated with maximum entropy, and that both the coma and seizure extremes have reduced entropy (increased order). While this is an intuitively attractive result, the supporting evidence is sparse at present. The work of Viertiö-Oja and colleagues [22] shows that spectral entropy does diminish during anesthetic induction (see [9] for further details), but, to our knowledge, the corresponding spectral entropy changes for the traversal into epileptic seizure have not yet been reported in the literature. Our own preliminary measurements for epileptic EEG suggest that spectral entropy is lowered in the seizure state. These early findings indicate that the large-c_1 LB entropy graph of Fig. 6(c) is at least plausible.

We note that for both Haken and LB forms there is an abrupt and discontinuous negative change in the macrocolumn entropy at the A_3 point of induction. A step change in entropy, ΔS, is characteristic of a first-order thermodynamic phase transition, and implies the existence of an analogous ''latent heat,'' $\Theta \Delta S$, for the cortex. The detection of this latent effect should provide a direct clinical means by which we can determine the amount of energy which must be removed from each macrocolumn in order to transform the cortex from a depolarized, disordered, conscious state to a hyperpolarized, ordered, hypnotic state.

G. Cortical ''heat capacity'' and ''latent heat''

For a thermodynamic system consisting of a sample and its environment, the *heat capacity* of the sample is the energy required to raise the temperature of the sample by 1 K. This is a ''heating'' experiment in which energy flows inwards, from the environment to the sample. Equivalently, heat capacity can be determined in a ''cooling'' experiment which measures the energy required to lower the temperature of the sample by 1 K; in this case the energy flow is outwards, from the sample to its environment. For the cortex, we seek to design an experiment which measures the outflow of energy from the cortex as it is ''cooled'' (its excitability reduced) under the influence of a general anesthetic.

The heat capacity depends on the *phase* or bonding structure of the sample. If the sample changes phase during the cooling experiment, then we should expect the change of phase to show up as an anomalous peak in the heat capacity. For a ferromagnetic substance cooled through its Curie temperature, the transition from the disordered, nonmagnetic state to the ordered, magnetically aligned state is smooth and continuous, and the transition is classified as second order. In contrast, the freezing of water and the cooling of a ferroelectric material through its Curie point are classified as first-order transitions, since both exhibit an abrupt and discontinuous change in order, quantifiable as a negative step change ΔS in entropy as the sample transforms from its liquid water (c.f. nonpolarized ferroelectric) disordered state to its ice-crystalline (c.f. polarized ferroelectric) ordered state. This discontinuous change in entropy is detectable as a sudden release of latent energy equal to $|T_c \Delta S|$, where T_c is the temperature at transition.

Our model of the cortex predicts that as anesthetic effect is increased, the soma voltage h_e and associated free energy V will change abruptly at a critical value for anesthetic effect λ. If the unconscious state is the more ordered, then the entropy change for the transition from the disordered, conscious state to the well-ordered, unconscious state will be negative, and latent energy should be *released* at the instant of transition. However, because of the uncertainty introduced by the presence of subcortical noise, we would not expect all 10^5 macrocolumns of the cortex to jump simultaneously (the larger the noise input into a given macrocolumn, the larger the probability that it will jump ''early''). Instead, the downward jumps into unconsciousness will occur over the noise-broadened range $\lambda_1 < \lambda < \lambda_{\text{jump}} < _{A_3}$, where $\lambda_1 > 1.0$ and $\lambda_{A_3} = 1.53$ (see Fig. 1). For small subcortical noise, $\lambda_{1,\text{jump}} \rightarrow 1.53$ and the transition range will be quite narrow; for large subcortical noise, the transition range will be comparatively broad.

What are the requirements for the definitive thermodynamics experiment applied to the anesthetic-damped cortex? Essentially we need to know how the energy uptake of the cortex varies as a function of anesthetic concentration. Ideally there would be simultaneous recordings of the EEG wave forms in order to correlate cortical electrical activity with cortical energy consumption as the brain moves into comatose unconsciousness.

We were very gratified to discover recently that the experiment we seek was performed over 20 years ago by Stullken *et al.* [23] (albeit for purposes quite different to ours). Stullken and colleagues were investigating the response of the cerebral metabolic rate for oxygen (CMR_{O_2}) in dogs to increasing concentrations of four different anesthetic agents: halothane, enflurane, isoflurane, and thiopental. Cerebral oxygen consumption was determined by measuring the change in blood oxygen concentration for blood entering and leaving the cerebral hemispheres, then multiplying this difference by the cerebral blood flow rate. The shapes of the anesthetic dose-response curves for CMR_{O_2} were examined by multiple measurements made at small, progressive concentration increments. For example, the six dogs in the halothane group received increasing concentrations of halothane such that the measured end-tidal (end-of-breath) concentration increased at a rate of 0.05% (of atmospheric pressure) every 5 min to 1.1%, and thereafter, at increments of 0.10% every 5 min. The EEG was continuously recorded and changes in EEG patterns from ''awake'' to ''anesthetic'' were correlated with changes in anesthetic concentration and CMR_{O_2}. The points of EEG change for awake to transitional ''shifting'' patterns, and from shifting to anesthetic patterns were determined by inspection of rhythm, amplitude, and frequency. High-frequency, low-amplitude activity (15 ± 5 Hz, 50 ± 40 μV) was classified as an awake pattern, while the onset of persistent lower-frequency and higher-amplitude activity (10 ± 8 Hz, 300 ± 150 μV) was classified as an anesthetic pattern. Shifting patterns showed alternation between awake and anesthetic characteristics.

Prior to the Stullken *et al.* experiment, it had been assumed that there was a linear negative-slope relationship be-

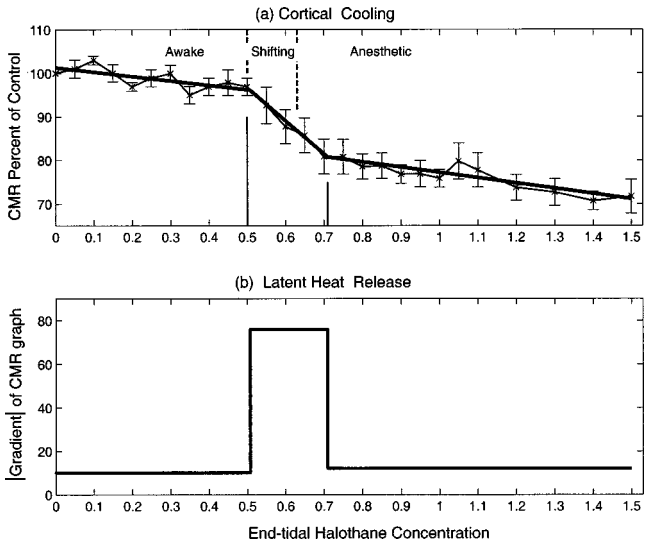

FIG. 7. Effect of general anesthetic (halothane) on the cerebral metabolic rate (CMR via oxygen consumption) for a dog, as reported by Stullken *et al.*, 1977 (refer to Fig. 3 of [23]). (a) CMR (as percent of control) is plotted versus end-of-exhalation halothane concentration (as percent of atmospheric pressure). Regression lines for changes in metabolic rate are drawn for each EEG-determined region. (b) We computed the negative slope of the regression lines of (a) to give the rate of decrease of metabolic rate with increasing anesthetic. The abrupt change in metabolic sensitivity to an anesthetic during the transition stage is very suggestive of a ''latent heat'' effect signaling a change of phase to the more ordered state.

tween the cerebral oxygen consumption (CMR_{O_2}) and the anesthetic concentration, but these earlier inferences of linear dose response had been based on a small number of isolated measurements. In contrast, Stullken's careful and detailed study revealed that CMR_{O_2} dose-response curves are nonlinear at anesthetic concentrations less than 1 MAC (minimum anesthetic concentration at which half the subjects are unresponsive to surgical incision; the MAC is a standard measure of anesthetic potency). For all four anesthetic agents studied (three inhalational, one intravenous), Stullken found that CMR_{O_2} decreased precipitously until a stable anesthetic EEG pattern was observed; thereafter CMR_{O_2} decreased only slowly. These results demonstrate that the change in the EEG pattern from awake to anesthetic is accompanied by an abrupt metabolic depression, and the researchers speculated that these events coincide with the onset of functional depression (loss of conscious awareness). The Stullken graph for the variation of metabolic rate with halothane concentration is shown in Fig. 7(a).

It is pertinent to emphasize an important distinction between a ''standard'' thermodynamics cooling experiment designed to determine the heat capacity of a closed, thermally insulated physical sample and the biological experiment performed by Stullken and co-workers. In the latter case, the ''sample'' is the living and metabolizing cortex of a dog which is necessarily an energy-dissipative, open system. In order to maintain an equilibrium state of the cortex, there must be a continuous flux of energy (oxygen plus nutrients) from the arterial blood to the cortex, and then from the cortex to the venous blood (metabolic waste products). As discussed in the Introduction, this molecular metabolic activity is occurring at spatial and temporal scales several orders of magnitude below that of our model, and serves to maintain the macrocolumn in its (local) equilibrium state. We picture the biological system as analogous to a nonideal ''lossy'' physical system.

A reasonable working definition for ''heat capacity'' of a dissipative biological system such as the cortex might be ''the amount by which the metabolic rate must change in order to change, by one unit, the state of excitability of the cortex,'' where ''excitability'' is an inverse measure of the anesthetic effect (see Sec. III E). This definition implies that it is the rate of energy delivery which determines the state of the neuron, whereas in fact the causality is the other way around: it is the state of the cell, as set by the anesthetic concentration, which determines the metabolic requirement and hence the blood flow. With this caveat in mind, we will apply this working definition to the Stullken experiment.

The halothane results of the Fig. 7(a) show that the overall trend is for the metabolic rate to diminish as the anesthetic depth increases. The gradient of this graph is negative, and its magnitude gives the percentage reduction in metabolic rate per unit increase in halothane concentration, or equivalently, per unit *decrease* in excitability (assuming an inverse relationship between halothane concentration and cortical excitability). Thus the slope magnitude can be interpreted as a cortical heat capacity; see Fig. 7(b).

Unlike the awake and anesthetic regions that have similar (gentle) slopes and therefore similar heat capacities, the intermediate shifting region has a dramatically steeper slope. This is the heat capacity anomaly which signals the thermodynamic phase change from the high-firing, high-metabolic-rate upper branch to the low-firing, low-metabolic-rate quiescent branch. The area of the anomaly gives the average decrease in the rate of energy consumption ($\approx 14\%$) during transition. We may also interpret this area as a measure of the rate of latent energy release from the cortex arising from the loss of entropy (gain in order) as the cortex transits to its unconscious state. Thus, during transition, the metabolic requirements of the cortex are offset by the latent energy which becomes available to the cortex as it ''crystallizes'' into hyperpolarized order.

In order to compare the Stullken experimental results with the model predictions for a single macrocolumn, we will focus on the excitatory neuron population (inhibitory results are very similar), assuming the Lugiato and Bonifacio form for free energy, and taking a ''temperature'' mapping $\Theta = c_0/\lambda^{c_1}$, with $c_0 = c_1 = 1.0$. This gives the LB entropy trajectory for induction shown in Fig. 8(a) which lies between those shown in Fig. 6(b) ($c = 0.2$) and Fig. 6(c) ($c = 3$).

Applying the assumed temperature mapping to the definition for the cortical heat capacity listed in Table II, we obtain

$$C = \Theta \frac{\partial S}{\partial \Theta} = -\lambda \frac{\partial S}{\partial \lambda}. \tag{3.7}$$

The resulting single-macrocolumn heat capacity is shown in

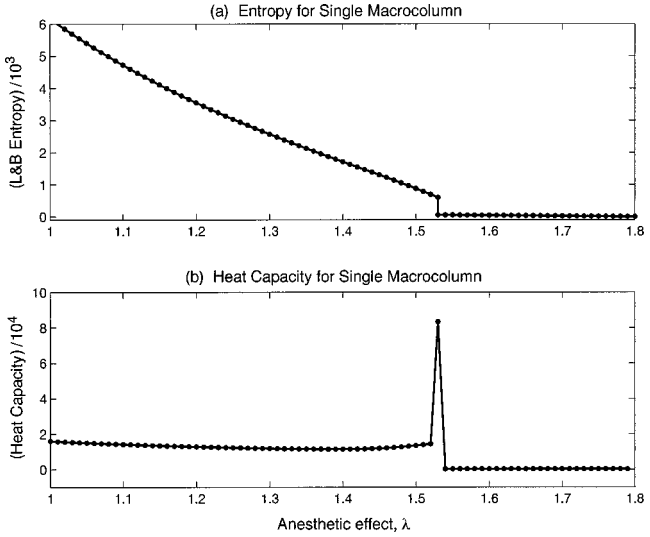

FIG. 8. Predicted variation in (a) entropy and (b) heat capacity for the excitatory neurons of a single macrocolumn during induction of anesthesia. The entropy curve assumes a simple inverse mapping between excitability (''temperature'') and the anesthetic effect: $\Theta = 1/\lambda$, and follows the Lugiato and Bonifacio scheme for free energy [see Eqs. (3.1) and (3.5c)]. The heat capacity is computed from the derivative of the entropy curve, $C = -\lambda(\partial S/\partial\lambda)$. The negative step discontinuity in entropy at $\lambda = 1.53$ produces a positive δ function in the heat capacity which we approximate as a triangular spike of area $1.53|\Delta S|$ and half-width equal to the sampling resolution of λ.

Fig. 8(b). As expected, the step decrease in entropy produces a heat-capacity anomaly corresponding to the release of latent heat as the model ''freezes'' into its hyperpolarized state. Only a single latent-heat spike is shown. This narrow peak would be expected to broaden if the contributions of all 10^5 macrocolumns participating in the CMR_{O_2} blood flow experiment could be summed, taking into account the expected variability for the various biological parameters (threshold voltage, input spike rates, noise amplitudes, etc.), but we note that we have not yet attempted multimacrocolumn modeling. Nevertheless, this apparent similarity between our preliminary theory and the clinical experiment is very encouraging.

In the following paper [9] we describe another test of model prediction versus clinical results. This second test will use spectral entropy to compare the spectral flatness of the theoretical fluctuation spectrum against that measured from EEG records for patients undergoing general anesthesia.

IV. SUMMARY AND CONCLUSIONS

In this paper we have linked the general-anesthetic phase transition of the cerebral cortex with thermodynamic phase transitions by drawing an analogy with the canonical ensemble of statistical mechanics. We view the applied anesthetic as an infinite bath which determines the internal energy and polarization of the cortex in much the same way as thermodynamic temperature determines the state of spontaneous polarization of a ferroelectric crystal.

This lead us to identify a parameter we named *excitation* (Θ), oppositely proportional to the anesthetic effect (λ), to serve as a temperature analog. By positing a set of simple but plausible (Θ,λ) inverse mappings, we were able to compute the analogous entropy and ''heat''-capacity changes for induction into unconsciousness, and for reemergence into consciousness. The theory predicts that the macrocolumn entropy S will decrease discontinuously at the active-to-quiescent transition, consistent with a first-order phase transition to a more ordered state. A second prediction is that the analogous heat capacity will diverge by an amount $|\Theta\Delta S|$ at transition, signaling the release of latent energy at the change of phase.

Detailed clinical measurements by Stullken *et al.* [23] of the changing metabolic requirements of the cortex during induction of anesthesia seem to be consistent with our theoretical picture of a phase change with latent energy release. This is a very encouraging finding.

Part of the motivation for invoking a canonical ensemble formalism is that once one has identified a temperature analog for the cortex, in principle, one could begin the task of enumerating cortical microstates and constructing a PDF for these microstates.

[1] M. L. Steyn-Ross, D. A. Steyn-Ross, J. W. Sleigh, and D. T. J. Liley, Phys. Rev. E **60**, 7299 (1999).
[2] K. Kuizenga, C. J. Kalkman, and P. J. Hennis, Br. J. Anaesth. **80**, 725 (1998).
[3] M. Bührer *et al.*, Anesthesiology **77**, 226 (1992).
[4] M. B. MacIver, J. W. Mandema, D. R. Stanski, and B. H. Bland, Anesthesiology **84**, 1411 (1996).
[5] D. P. Archer and S. H. Roth, Br. J. Anaesth. **79**, 744 (1997).
[6] P. Glansdorff and I. Prigogine, *Thermodynamic Theory of Structure, Stability, and Flutuations* (Wiley-Interscience, New York, 1974).
[7] L. A. Lugiato and R. Bonifacio, in *Coherence in Spectroscopy and Modern Physics*, edited by F. T. Arecchi, R. Bonifacio, and M. O. Scully, NATO Advanced Study Institute, Series B: Physics, Vol. 37 (Plenum, New York, 1978), pp. 85–109.
[8] H. Haken, *Synergetics: An Introduction: Nonequilibrium Phase Transitions and Self-organization in Physics* (Springer-Verlag, Berlin, 1978).
[9] D. A. Steyn-Ross, M. L. Steyn-Ross, L. C. Wilcocks, and J. W. Sleigh, following paper, Phys. Rev. E **64**, 011918 (2001).
[10] D. T. J. Liley, P. J. Cadusch, and J. J. Wright, Neurocomputing **26-27**, 795 (1999).
[11] C. W. Gardiner, *Handbook of Stochastic Methods for Physics, Chemistry, and the Natural Sciences*, Springer Series in Synergetics Vol. 13 (Springer-Verlag, Berlin, 1985).
[12] L. Ingber, Physica D **5**, 83 (1982).
[13] L. Ingber, Phys. Rev. A **45**, 2183 (1992).
[14] H. M. Gibbs, *Optical Bistability: Controlling Light with Light* (Academic Press, Orlando, 1985).
[15] R. Graham, *Quantum Statistics in Optics and Solid-State Phys-*

ics, Springer Tracts in Modern Physics Vol. 66 (Springer-Verlag, New York, 1973).

[16] N. P. Franks and W. R. Leib, Nature (London) **367**, 607 (1994).

[17] M. V. Jones, P. A. Brooks, and N. L. Harrison, J. Physiol. (London) **449**, 279 (1992).

[18] C. Kittel, *Introduction to Solid State Physics*, 7th ed. (Wiley, New York, 1996).

[19] A. v. Zeil, *Solid State Physical Electronics*, 2nd ed. (Prentice-Hall, London, 1968).

[20] M. E. Lines and A. M. Glass, in *Principles and Applications of Ferroelectrics and Related Materials*, edited by W. Marshall and D. H. Wilkinson, International Series of Monographs on Physics (Clarendon Press, Oxford, 1977).

[21] E. Fatuzzo and W. J. Merz, in *Ferroelectricity*, edited by E. P. Wohlfarth, Selected Topics in Solid State Physics Vol. 7 (North-Holland, Amsterdam, 1967).

[22] H. E. Viertiö-Oja, *et al.*, J. Clin. Monit. Comput. **16**, 60 (2000).

[23] E. H. Stullken, Jr., J. H. Milde, J. D. Michenfelder, and J. H. Tinker, Anesthesiology **46**, 28 (1977).